samples. Each run was performed in at least duplicate, and each sample was analyzed at least twice by capillary GC. In the presence of 5.0 M 2,3-dimethyl-1,3-butadiene (quencher) the photocycloaddition of dienone **4a** (4.7 mM) was quenched by 27% after 2 h of irradiation. In the presence of 2.3 M biphenyl (quencher) the photocycloaddition of dienone **4a** (1.4 mM) was quenched by 14% after 2 h of irradiation. Irradiation of dienone **5a** (3.9 mM) in the presence of 4.1 M 2,3-dimethyl-1,3-butadiene for 70 h showed no quenching of the photocycloaddition reaction.

Sensitization Studies of Dienones 4a, 4b, 5a, and 5b. Benzene solutions (~3 mL) containing dienone (1.9–7.1 mM), sensitizer (10–20 mM), and an internal standard (nonane) were prepared so that the sensitizer absorbed all the light in the portion of the spectrum where the dienone absorbed. The samples were irradiated ($\lambda \geq 280$ nm) using the merry-go-round set up concurrently with control samples which contained identical concentrations of dienone but no sensitizer. All samples were run in at least duplicate and analyzed by capillary GC.

Stereochemical Scrambling Studies. ^{1}H NMR samples of dienones **11a** and **12a** (~0.1 M in benzene-d_6) were irradiated at $\lambda \geq 280$ nm. The degree of scrambling was measured by integration of the appropriate C6 hydrogens NMR signals: **12a**, δ 5.08 vs 4.96; **11a**, δ 5.10 vs 5.01. The use of benzene-d_6 as solvent gave rise to large changes in chemical shift that permitted the separation of signals in the vinyl region. The key vinyl protons that needed to be integrated were doublets of triplets. In mixtures of the (*Z*)- and the (*E*)-deuterio isomers of the dienones one of the triplet pairs was partially obscured by overlapping resonances. Because the intensity of the two halves of the signal were not equal, a weighting factor was used to determine the correct integral value by measurement of one of the triplets of the dt multiplet. The weighting factors were determined from the highly enriched isomers. The ratio of the integrals of the two triplets was 56:44 in dienones **11a** and **12a** and in the *E* and *Z* deuterated allylic alcohols. The extent of conversion of dienone **12a** to photoproduct was monitored by the appearance of signals at δ 4.02 (1 H, d) and δ 3.42 (1 H, d). Dienone **11a** showed large amounts of scrambling of the label before any product could be observed by NMR. An estimated 5% of the product would have been accurately detected.

Acknowledgment. Acknowledgement is made to the donors of the Petroleum Research Fund, administered by the American Chemical Society, and Oberlin College for support of this work. We thank W. C. Agosta for helpful discussions and C. Y. Strohl for initial studies.

Supplementary Material Available: ^{1}H NMR spectra of **4a**, **4b**, **5a**, **5b**, **6a**, **6b**, **7**, **8**, **11a**, **11b**, **12a**, and **12b** and ^{13}C NMR spectra of **4a**, **6a**, **7**, and **8** (16 pages). This material is contained in many libraries on microfiche, immediately follows this article in the microfilm version of the journal, and can be ordered from the ACS; see any current masthead page for ordering information.

Stereoelectronic Effect of the Trimethylsilyl Substituent upon C–O Bond Lengths at the β Position: Some Structural Studies

Jonanthan M. White*,† and Glen B. Robertson

Research School of Chemistry, Australian National University, G.P.O. Box 4, Canberra, ACT 2601, Australia

Received December 26, 1991 (Revised Manuscript Received May 7, 1992)

Results of low-temperature (130 K) crystal structure analyses for seven β-trimethylsilyl-substituted cyclohexylnitrobenzoate esters are reported. For those molecules (three) with the Si–C and C–O bonds antiperiplanar the C–O bond lengths are increased by 0.014 Å av (Δ/σ min = 2.9) compared with that in the silicon-free analogue. For those molecules (four) with the Si–C and C–O bonds gauche no such systematic lengthening of the C–O bonds is observed. The result is in qualitative agreement with that [$\Delta l \propto \cos^2$ (Si–C–C–O)] predicted from semiempirical MO calculations on a simple model complex and is attributed to the effects of interactions between the Si–C σ and C–O σ^* orbitals. It is suggested that existence of the observed ground-state effect constitutes persuasive, if circumstantial, evidence that the major kinetic effects known to result from the presence of a β silicon substituent also have their genesis in the same σ–σ^* interactions.

Introduction

The ability of silicon to accelerate reactions which lead to the development of positive charge on a β carbon atom, the so called β effect, is pivotal to the chemistry of organosilicon compounds.[1,2] For example, the presence of β $SiMe_3$ has been shown, in stereochemically constrained systems, to enhance solvolysis rates (relative to β H) by a factor of 10^{12}.[3] In addition to its inductive effect, the $SiMe_3$ substituent is believed to stabilize the developing carbocation by one or other of two mechanisms (Scheme I). The first involves internal displacement of the leaving group to form the silacyclopropylium cation b and the second involves hyperconjugation of the C–Si σ bond with the unfilled β carbon p-orbital a. The relative importance of these two intermediates in systems containing primary β carbon atoms remains substantially unresolved.[2]

Recently, however, Lambert and co-workers, in a series of elegant experiments employing conformationally constrained systems based on 5- and 6-membered rings,[3,4] have demonstrated a marked dependence of reaction rate upon the Si–C–C–Lg dihedral angle (Lg = leaving group) and conclude that, at least in such secondary (carbon atom) systems, there is necessarily substantial involvement of the "open" cation a in the reaction pathway. The increasing

Scheme I. Stabilization of Positive Charge by β Silicon

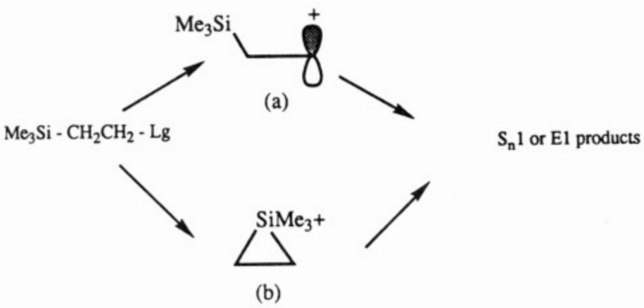

---

† Present address: Chemistry Department, University of Melbourne, Parkville, Victoria 3052, Australia.

(1) Colvin, E. *Silicon in Organic Synthesis*: Butterworths Monographs in Chemistry, Butterworth: Boston, 1981.

(2) Lambert, J. B. *Tetrahedron* **1990**, *46*, 2677.

(3) Lambert, J. B.; Wang, G.-T.; Finzel, R. B.; Teramura, D. H. *J. Am. Chem. Soc.* **1987**, *109*, 7838.

(4) Lambert, J. B.; Wang, G.-T. *J. Phys. Org. Chem.* **1988**, *1*, 169. Lambert, J. B.; Chelius, E. C. *J. Am. Chem. Soc.* **1990**, *112*, 8120.

0022-3263/92/1957-4638$03.00/0

evidence for the involvement of type a cations has led us to speculate on the possibility of there being observable ground-state effects due to a hyperconjugative type interaction between the C–Si σ-orbital and the C–Lg σ^*-orbital. Such effects might be expected to include weakening, by differing amounts, of both the C–Si and C–Lg bonds and strengthening of the central C–C bond. Like the probability of formation of the type a cations the bond-strength and any concomitant bond-length variations are also expected to be angle dependent, being maximal (probably unequal[5]) for Si–C–C–Lg dihedral angles of 0° and 180° and zero at 90°. The experimental observation of such effects in Si–C–C–Lg fragments would constitute persuasive, additional evidence for type a cations as the predominant reaction intermediates. Accordingly, we decided to prepare, and to perform structural studies on, a selection of conformationally constrained model compounds containing trimethylsilyl substituents β to the leaving groups. In model compounds **1**, **2**, and **3** the trimethylsilyl substituent is disposed anti to the leaving group (*p*-nitrobenzoate in **1** and **2**, 3,5-*m*-dinitrobenzoate in **3**) and in compounds **4**–**7** is disposed gauche to the *p*-nitrobenzoate leaving group. The model compounds were each prepared by esterification of the corresponding β trimethylsilyl alcohol (**8**–**13**).

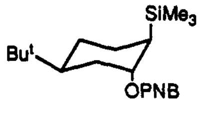

(1)

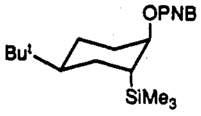

(2)

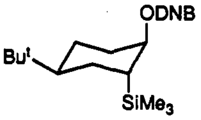

(3)

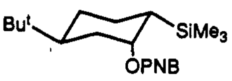

(4)

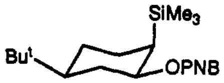

(5)

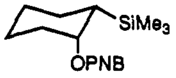

(6)

(7)

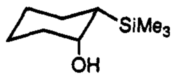

(13)

Scheme II

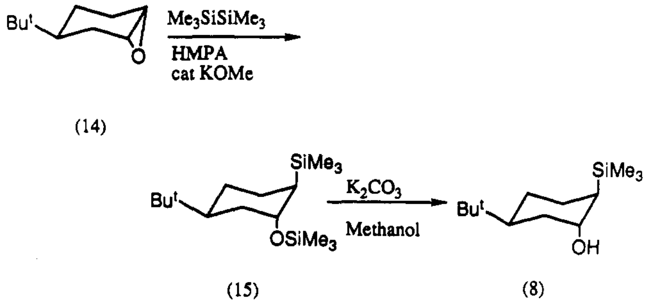

Scheme III

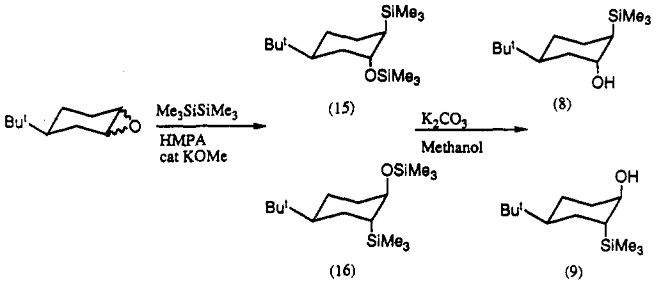

Scheme IV

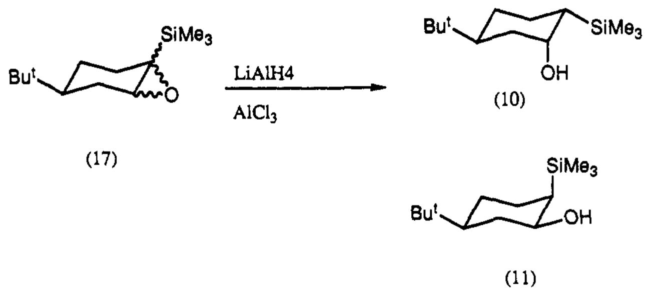

Scheme V

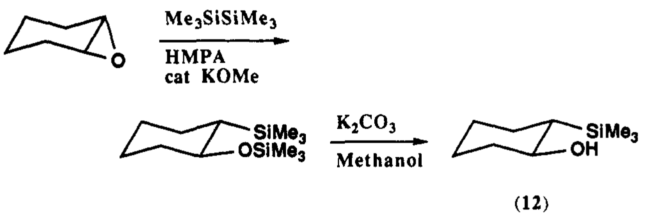

Results

Synthesis. Preparation of the 5-*tert*-butyl-*anti*-trimethylsilyl alcohol **8** was based on the method by Lambert et al.[3] (Scheme II), except that ring opening of the trans epoxide **14** was achieved using hexamethyldisilane in HMPA (HMPA = hexamethylphosphoramide) with a catalytic quantity of potassium methoxide.[6] The 4-*tert*-butyl analogue **9** was prepared by ring opening of a mixture of *cis*- and *trans*-4-*tert*-butylcyclohexene oxides as described for **8** (Scheme III). Deprotection of the resulting trimethylsilyl ethers **15** and **16** gave a 1:1 mixture of the alcohols **8** and **9**, from which **9** was obtained pure by fractional crystallization. The gauche silyl alcohols **10** and **11** were prepared by ring opening of a mixture of the *cis*- and *trans*-4-*tert*-butyltrimethylsilyl epoxides **17** as previously described[3] (Scheme IV) to give a mixture of the alcohols **10** and **11**. These were separated readily by column chromatography. The gauche trimethylsilyl alcohol **12** was prepared by ring opening of cyclohexeneoxide using hexamethyldisilane in HMPA with a catalytic amount of potassium methoxide as described above (Scheme V). The remaining gauche trimethylsilyl alcohol **13** was prepared as previously reported.[3] Conversion of the alcohols **8**–**13** to the corresponding esters **1**–**7** was achieved by standard methods.

Molecular Structures

The molecular structures of compounds **1**–**7**, all determined at 130 K in order to reduce unwanted thermal effects, are shown in Figures 1–7. The figures were drawn with ORTEP and depict 50% ellipsoids.[7] Hydrogen atoms, for which thermal parameters were constrained to be isotropic, have been omitted for clarity. Selected bond

---

(5) David, S.; Eisenstein, O.; Hehre, W. J.; Salem, L.; Hoffman, R. *J. Am. Chem. Soc.* **1973**, *95*, 3806. Inagaki, S.; Iwase, K.; Mori, Y. *Chem. Lett.* **1986**, 417.

(6) Dervan, P. B.; Shippey, M. A. *J. Am. Chem. Soc.* **1976**, *98*, 1265.

(7) Johnson, C. K. ORTEP-II, Report ORNL-5138; Oak Ridge National Laboratory, Oak Ridge, TN, 1976.

Table I. Selected Bond Lengths (Å) and Interbond Angles (deg) for Compounds 1–7

	1	2	3	4	5	6	7
O(1)–C(2)	1.490 (2)	1.483 (3)	1.487 (3)	1.476 (3)	1.476 (2)	1.474 (5)	1.467 (3)
C(1)–C(2)	1.515 (2)	1.526 (3)	1.527 (3)	1.524 (3)	1.525 (3)	1.531 (5)	1.525 (3)
Si–C(1)	1.902 (1)	1.898 (3)	1.901 (3)	1.896 (2)	1.898 (2)	1.892 (3)	1.894 (2)
Si–CH_3 (av)	1.865	1.866	1.867	1.862	1.862	1.863	1.865
Si–C(1)–C(2)	113.3 (1)	113.2 (2)	112.4 (2)	115.2 (1)	119.4 (2)	115.2 (2)	117.3 (2)
Si–C(1)–C(6)	116.0 (1)	117.9 (2)	116.4 (2)	113.1 (1)	115.3 (2)	114.3 (2)	109.1 (2)
O(1)–C(2)–C(1)	107.2 (1)	109.0 (2)	110.1 (2)	106.5 (2)	111.3 (2)	104.6 (3)	106.3 (2)
O(1)–C(2)–C(3)	107.0 (1)	105.7 (2)	105.3 (2)	107.4 (2)	106.0 (2)	109.1 (3)	109.6 (2)
C(1)–C(2)–C(3)	114.1 (1)	113.7 (2)	113.9 (2)	113.5 (2)	114.1 (2)	113.8 (3)	113.0 (2)
C(2)–C(3)–C(4)	113.0 (1)	113.3 (2)	113.5 (2)	113.2 (2)	110.6 (2)	112.8 (3)	110.0 (2)
C(3)–C(4)–C(5)	108.4 (1)	111.1 (2)	111.0 (2)	108.6 (2)	108.9 (2)	110.8 (3)	111.3 (2)
C(4)–C(5)–C(6)	111.9 (1)	108.2 (2)	106.9 (2)	111.0 (2)	111.6 (2)	111.2 (3)	110.6 (2)
C(5)–C(6)–C(1)	113.2 (1)	113.8 (2)	112.4 (2)	112.7 (2)	113.2 (2)	112.2 (3)	112.1 (2)
C(6)–C(1)–C(2)	110.9 (1)	111.6 (2)	111.5 (2)	110.4 (2)	106.3 (2)	110.4 (3)	108.8 (2)

Table II. Selected Dihedral Angles for Compounds 1–7

	1	2	3	4	5	6	7
Si–C(1)–C(2)–C(3)	83.7 (1)	–89.6 (2)	87.4 (2)	179.2 (1)	75.9 (3)	177.7 (3)	–179.8 (2)
Si–C(1)–C(6)–C(5)	–81.1 (1)	81.9 (2)	–76.8 (2)	176.8 (1)	–80.1 (2)	–175.0 (3)	175.8 (2)
Si–C(1)–C(2)–O(1)	–158.0 (1)	152.7 (2)	–154.5 (2)	61.3 (2)	–44.0 (3)	–63.4 (3)	–59.6 (2)
O(1)–C(2)–C(3)–C(4)	–65.1 (1)	70.4 (2)	–74.1 (2)	64.4 (2)	–177.2 (2)	–64.3 (4)	–175.2 (2)
O(1)–C(2)–C(1)–C(6)	69.6 (1)	–71.5 (3)	72.7 (2)	–68.4 (2)	–176.5 (2)	67.9 (3)	176.0 (2)
C(1)–C(2)–C(3)–C(4)	53.4 (2)	–49.2 (3)	46.8 (3)	–53.0 (2)	60.0 (2)	52.1 (5)	–57.0 (3)
C(2)–C(3)–C(4)–C(5)	–55.5 (1)	55.7 (3)	–55.1 (3)	55.5 (2)	–56.3 (2)	–53.3 (5)	56.2 (3)
C(3)–C(4)–C(5)–C(6)	56.6 (1)	–58.1 (3)	60.7 (3)	–57.5 (2)	55.5 (3)	55.4 (5)	–56.3 (3)
C(4)–C(5)–C(6)–C(1)	–55.6 (2)	57.4 (3)	–61.1 (3)	57.8 (2)	–57.0 (3)	–56.4 (5)	56.2 (4)
C(5)–C(6)–C(1)–C(2)	50.0 (1)	–51.6 (3)	54.0 (3)	–52.3 (2)	54.6 (2)	53.2 (4)	–55.1 (3)
C(6)–C(1)–C(2)–C(3)	–48.7 (1)	46.2 (3)	–45.4 (3)	49.5 (2)	–56.6 (2)	–51.1 (4)	55.8 (3)

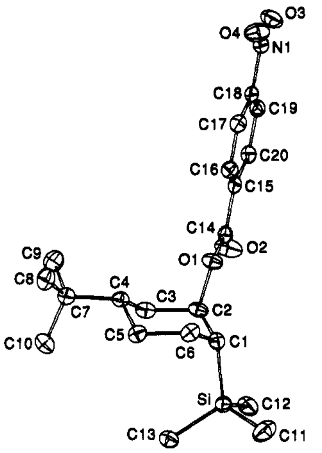

Figure 1. Structure of *r*-5-*tert*-butyl-*c*-2-(trimethylsilyl)cyclohex-*t*-yl *p*-nitrobenzoate (1).

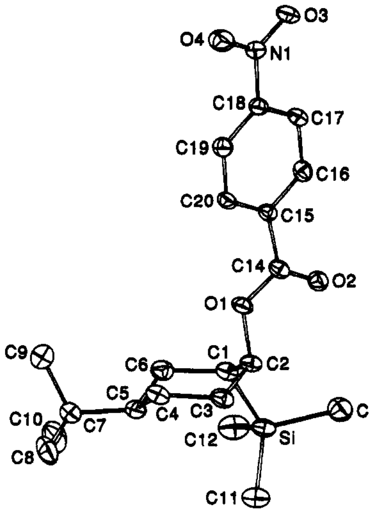

Figure 2. Structure of *r*-4-*tert*-butyl-*t*-2-(trimethylsilyl)cyclohex-*c*-yl *p*-nitrobenozate (2).

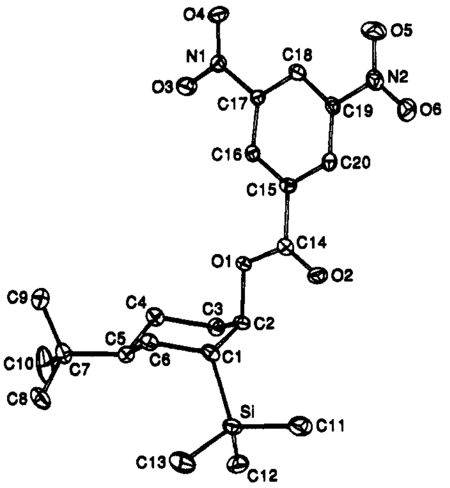

Figure 3. Structure of *r*-4-*tert*-butyl-*t*-2-(trimethylsilyl)cyclohex-*c*-yl 3,5-dinitrobenzoate (3).

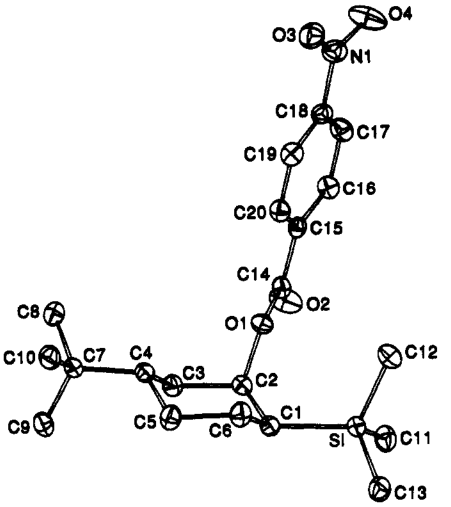

Figure 4. Structure of *r*-5-*tert*-butyl-*t*-2-(trimethylsilyl)cyclohex-*t*-yl *p*-nitrobenzoate (4).

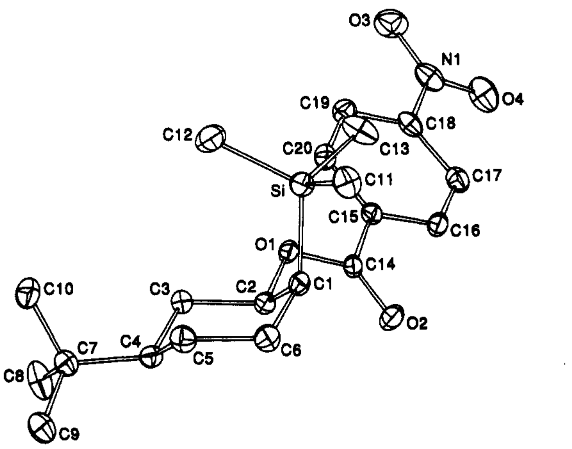

Figure 5. Structure of *r*-5-*tert*-butyl-*c*-2-(trimethylsilyl)cyclohex-*c*-yl *p*-nitrobenzoate (5).

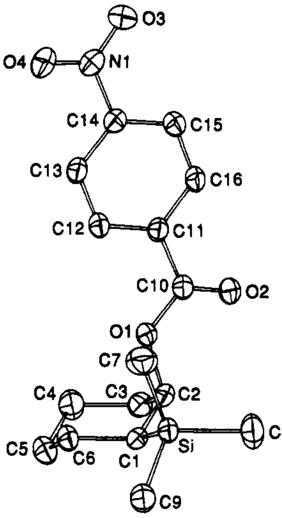

Figure 6. Structure of *cis*-2-(trimethylsilyl)cyclohexyl *p*-nitrobenzoate (6).

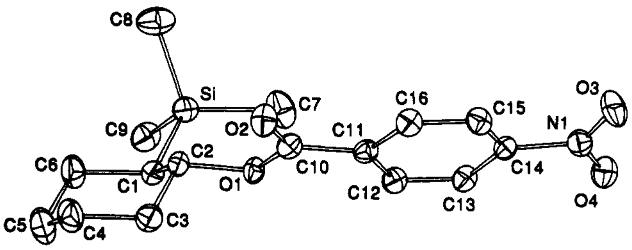

Figure 7. Structure of *trans*-2-(trimethylsilyl)cyclohexyl *p*-nitrobenzoate (7).

lengths and interbond angles are listed in Table I and selected dihedral angles are listed in Table II. Atomic coordinates and thermal parameters and complete bond length and bond angle listings are included in the supplementary material. Structures of the silicon-free compounds 18 and 19 have also been determined from 130 K data. Details will be reported elsewhere.

(18)

(19)

Inspection of Tables I and II confirms the presence of appreciable angle strain at the C(1), C(2), C(3), and C(6) cyclohexane carbon centers manifest, both, as a general flattening of the ring [e.g., the C(6)-C(1)–C(2)–C(3) angles] and a sometimes substantial opening of the Si–C–C angles. As a consequence the Si–C–C–O torsion angles in the anti compounds 1–3 are each reduced from 180° to ca. 155°. For the lone gauche compound with the trimethylsilyl substituent axial 5 the Si–C–C–O torsion angle is reduced, likewise, from −60° to −44°. Those gauche structures with the trimethylsilyl substituents equatorial (4, 6, 7) all exhibit Si–C–C–O angles quite close to the ideal value (61.3°, −63.2°, and −59.6°, respectively, cf. ±60°).

As is evident from Table I the O–C(cyclohexane)[O(1)–C(2)] bonds in the anti compounds 1–3 are slightly lengthened vis à vis their counterparts in the gauche compounds 4–7. No other systematic and significant bond length variations are observed across the entire range of complexes 1–7.

Discussion

Whereas the C–O(ester) bonds in structures 1–4 and in 6 are each axial, those in structures 5 and 7 are equatorial. Bond length differences in the anti (1–3) and gauche (4–7) structures are small [Δ(C–O) max/min 0.23 (4)/0.07 (4) Å], and it becomes important to take proper account of the natural difference, if any, between axial and equatorial C–O(ester) bonds. To this end, we have determined, also at 130 K, the structures of the silicon-free molecules 18 and 19.[8] The C–O bond length in the axial *p*-nitrobenzoate 18 is 1.473 (2) Å, cf. a mean value of 1.466 (1) Å (two independent molecules; l = 1.464 (2), 1.468 (2) Å) in the equatorial ester 19.[9] The C–O bond lengths for the anti structures 1–3, with axial *p*-nitrobenzoate groups, are all significantly lengthened (Δ/σ min = 2.9) relative to that in the silicon-free axial ester 18, while the C–O bond lengths in the gauche structures 4 and 6, which also have axial *p*-nitrobenzoate groups, are essentially the same as in 18. The C–O bond lengths in the equatorial *p*-nitrobenzoate gauche structure 7 [1.467 (3) Å] is, likewise, essentially the same as that in its equatorial silicon-free analogue 19. However, the gauche structure 5, which also has the *p*-nitrobenzoate equatorial, has a C–O bond length [1.476 (2) Å] significantly greater than that in 19.

The above observations are consistent with the expectation of weakening, and hence lengthening, of the C–O(ester) bonds due to the presence of ground-state hyperconjugative type (C–Si) σ– (C–O) σ^* interactions. The bond lengthening is greatest for those structures 1–3 (ca. 0.014 Å av) where the C–Si bond is close to antiperiplanar to the C–O bond (Si–C–C–O ca. 155°) and is insignificant for those structures 4, 6, and 7 where the dihedral angle is close to 60°. The observed lengthening of the C–O bond in 5 relative to that in 19 (ca. 0.01 Å) is unexpected. The O–C(carboxylate) bond [O(1)–C(14)] is also lengthened by about the same amount (relative to those in 7 and in 19) suggesting either experimental artifact or, more likely, crystal packing effects.

We have performed semiempirical MO calculations (AM1)[14] on the simple model compound 20 in which a SiH_3

---

[8] White, J. M.; Robertson, G. B. Manuscript in preparation.

[9] C–O distances in R^1–O–R^2 fragments are dependent on the natures of both R^1 and R^2.[10] Literature values directly comparable with those in 18 and 19, but derived from room-temperature analyses, are: 1.466 (3) Å in *trans*-2-hydroxycyclohexyl *p*-nitrobenzoate[11] [cf. 1.473 (3) Å in 18] and 1.467 and 1.462 (3) Å in 2-hydroxy[4.2.2]propellanyl *p*-nitrobenzoate[12] and (1*R**,9*S**,10*S**)-5,5,9-trimethyldecahydro-1-naphthyl *p*-nitrobenzoate,[13] respectively [cf. 1.466 (2) Å in 19].

[10] Allen, F. H.; Kirby, A. J. *J. Am. Chem. Soc.* 1984, *106*, 6197.

[11] Jones, P. G.; Edwards, M. R.; Kirby, A. J. *Acta Crystallogr., Sect. C* 1989, *C45*, 249.

[12] Silverton, J. V.; Milne, G. W. A.; Eaton, P. E.; Nyi, K.; Temme, G. H. *J. Am. Chem. Soc.* 1974, *96*, 7429.

[13] Scheller, M. E.; Mathies, P.; Petter, W.; Frei, B. *Helv. Chim. Acta* 1984, *67*, 1748.

substituent is β to a protonated hydroxyl leaving group.

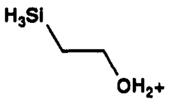

(20)

The model calculations show that (i) relative to their values at θ ca. 90° (θ = Si–C–C–O dihedral angle) the Si–C/C–O bond lengths are elongated by 0.036/0.029 Å at $\theta = 180°$ and by 0.006/0.009 Å at $\theta = 0°$, (ii) the C–C distance contracts by 0.022 Å at 180° and by 0.006 Å at 0°, (iii) in the separate ranges 0–90° and 90–180° the length/angle dependence is approximately as $\cos^2 \theta$ ($\sin^2 \theta$ for C–C), and (iv) the Si–C/C–O bond lengths for the gauche conformation (1.888/1.528 Å) are not sensibly different to those for $\theta = 90°$ (1.889/1.529 Å), for which angle the σ–σ^* interaction should be zero. Except for structure **5**, there is good qualitative agreement between the predicted and observed behavior of the C–O distances, with negligible lengthening being observed in the gauche structures **4**, **6**, and **7**, but significant lengthening in the anti structures **1**–**3** (Δl_{obsd} 0.014 Å av; Δl_{calcd} for **20** 0.026 Å). For the Si–C and C–C distances the correlation is altogether less good, with observed lengthenings for the anti, cf. gauche, complexes of only +0.005 Å av and −0.003 Å av, respectively, compared with predicted changes for **20** of +0.033 and −0.017 Å.

It is a well established fact that changes of a few hundredths of an angstrom in C–O bond lengths can markedly affect the rates of heterolysis of those bonds.[15,16] We do not have kinetic data for any of the complexes **1**–**7** but rate enhancements for the anti and gauche *tert*-butyl-β-silylcyclohexyl trifluoroacetates **21** and **22**, relative to cyclohexyltrifluoroacetate, have been shown by Lambert et al.[3] to be, respectively, 2.4×10^{12} and 3.3×10^4. These data, in conjunction with the bond length data from structures **1**–**7**, are clearly consistent with a causal relationship between weakening of the C–O bond in the ground state due to the σ–σ^* interaction and the enhanced solvolysis rate with β-silicon substituents. As the C–O bond lengthens, in proceeding along the reaction coordinate from the ground to the transition state, the σ–σ^* interaction is likely to be enhanced dramatically due to the decrease in the C–O σ^* energy level and the concomitant improvement in energy match with the Si–C σ orbital leading, finally, to dissociation to the type a cation.

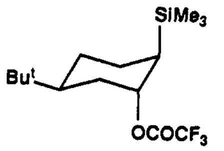

(21)

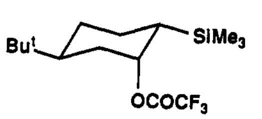

(22)

Providing that the solvolysis reaction does, indeed, proceed via the type a cation pathway then, according to Lambert et al., the stereochemical dependence of the rate acceleration should be given by

$$\log (k_{\mathrm{Si},\theta}/k_{\mathrm{H}}) = \cos^2 \theta\, [\log (k^{\mathrm{V}}_{\mathrm{Si},0°}/k^{\mathrm{V}}_{\mathrm{H}})] + \log (k^{\mathrm{I}}_{\mathrm{Si}}/k^{\mathrm{I}}_{\mathrm{H}})$$

where $k_{\mathrm{Si},\theta}$ is the observed rate for the silylated molecule with Si–C–C–O dihedral angle equal to θ, k_{H} is that for the unsilylated molecule, and V and I denote hyperconjugative (vertical) and inductive contributions, respectively. Lambert et al. have made use of this equation to estimate the separate V and I contributions to the rate enhancements for **21** and **22**. With θ assumed equal to 180° and 60° for **21** and **22**, respectively, they calculate a (common) inductive contribution of 1×10^2 and vertical contributions of 2.4×10^{10} for **21** and 3.3×10^2 for **22**. They observed, too, that a data fit can also be obtained with the inductive contribution assumed to be zero but only at the expense of very large deviations of the θ values from 60 or 180° (e.g., $\theta = 60°$ for **22** requires $\theta = 145°$ for **21**). The present results suggest a situation intermediate between these two extremes. The θ value for structures **1**–**3** averages 155.1° with no evident systematic difference between the *p*-nitrobenzoate complexes **1** and **2** and the *m*-dinitrobenzoate complex **3**. In each instance the ca. 155° θ value is apparently a consequence of the need to minimize 1,3 diaxial interactions between the substituent groups and the ring hydrogen atoms. Moreover, given that the *A* value for *p*-nitrobenzoate (0.9 kcal/mol)[17] is not a lot larger than that for trifluoroacetate (0.68 kcal/mol)[18] it seems highly probable that the θ value for **21** will be close to those for structures **1**–**3**. For assumed θ values of 155° for **21** and 62.5° (av for structures **4** and **6**) for **22** the estimated inductive acceleration becomes 75 and the estimated vertical acceleration when $\theta = 180°$ becomes 6.2×10^{12}. With θ assumed equal to 60° for **22** the estimated inductive acceleration is further reduced to 16.

Conclusion

The present structural data provide direct evidence that the presence of a silyl substituent β to a C–O(ester) linkage can lengthen and hence weaken the C–O bond in the molecular ground state. The observed lengthening is greatest (av 0.014 Å) in those structures (**1**–**3**) in which the C–Si and C–O bonds are antiperiplanar and is negligible in those structures (**4**–**7**) in which the C–Si and C–O bonds are gauche. We believe this to be the result of σ–σ^* interactions in which the C–Si σ-bonding orbital acts as the donor and the C–O σ^* orbital acts as the acceptor. The observed angular dependence of the ground-state effect is both matched by, qualitatively, and provides a rationale for the widely different solvolysis rates observed for the anti and gauche *tert*-butyl-β-silylcyclohexyl trifluoroacetates **21** and **22**.[3] The same effect serves, also, to explain the observed decrease in reactivity of a leaving group with a syn, cf. antiperiplanar, silyl substituent at the β position since σ–σ^* interactions are predicted to be smaller for the syn than for the antiperiplanar arrangement.

In summary, the structural data for complexes (**1**–**7**) provide a new insight into the origin of the silicon β effect and constitutes persuasive, if circumstantial, additional evidence that solvolysis of such complexes proceeds via the open cation a rather than via a type b silacyclopropylium intermediate.

Experimental Section

(a) Synthesis. Melting points were determined on a Gallenkamp melting point apparatus, and infrared spectra were run on a Perkin-Elmer 1800 fourier transform infrared spectrometer. NMR spectra were run on a Varian Gemini NMR spectrometer operating at 300 MHz for proton and 75 MHz for carbon spectra. NMR and spectral data have been deposited.

***r*-5-*tert*-Butyl-*t*-1-(trimethylsiloxy)-*c*-2-(trimethylsilyl)cyclohexane (15).** *trans*-4-*tert*-Butylcyclohexene oxide (1 g, 6.5 mmol) was added to a solution of hexamethyldisilane (2.4 g, 16 mmol) and potassium methoxide (100 mg) in HMPA (40 mL) at 55 °C. The resulting red-brown solution was stirred for

---

(14) Dewar, M. J. S.; Zoebisch, E. G.; Healy, E. F.; Stewart, J. J. P. *J. Am. Chem. Soc.* **1985**, *107*, 3902.

(15) Bürgi, H. B.; Dunitz, J. D. *Acc. Chem. Res.* **1983**, *16*, 153.

(16) Kirby, A. J.; Jones, P. G. *J. Am. Chem. Soc.* **1984**, *106*, 6207.

(17) Eliel, E. L. *Stereochemistry of Carbon Compounds*: McGraw Hill: New York, 1962.

(18) Hirsch, J. A. *Top. Stereochem.* **1967**, *1*, 199.

Table III. Crystal Data and Refinement Detail

compd	1	2	3	4	5	6	7
cryst. class	monoclinic	monoclinic	monoclinic	monoclinic	monoclinic	triclinic	monoclinic
a (Å)	18.731 (3)	18.030 (5)	18.703 (3)	14.032 (2)	18.318 (4)	6.379 (4)	6.951 (1)
b (Å)	18.465 (2)	9.784 (2)	11.788 (3)	6.625 (1)	6.523 (1)	12.436 (3)	35.359 (6)
c (Å)	6.1858 (5)	12.688 (3)	10.009 (1)	22.582 (3)	17.899 (4)	12.547 (4)	7.112 (1)
α (deg)	90	90	90	90	90	110.18 (2)	90
β (deg)	100.46 (1)	107.90 (2)	91.84 (2)	98.82 (2)	102.54 (2)	103.78 (3)	103.37 (1)
γ (deg)	90	90	90	90	90	102.50 (4)	90
space gp	$P2_1/n^a$	$P2_1/c$	$P2_1/c$	$P2_1/c$	$P2_1/n^a$	$P\bar{1}$	$P2_1/n^a$
M_r	377.55	377.55	422.55	377.55	377.55	321.45	321.45
ρ_c (g cm^{-3})	1.245	1.18	1.27	1.20	1.20	1.24	1.26
Z	4	4	4	4	4	2	4
crystal dimensns (mm)	0.20 × 0.24 × 0.32	0.30 × 0.30 × 0.30	0.28 × 0.22 × 0.20	0.28 × 0.12 × 0.10	0.28 × 0.22 × 0.15	0.24 × 0.30 × 0.06	0.32 × 0.07 × 0.04
temp (K)	130	130	130	130	130	130	130
radiation	CuK$\bar{\alpha}$	MoK$\bar{\alpha}$	MoK$\bar{\alpha}$	MoK$\bar{\alpha}$	MoK$\bar{\alpha}$	CuK$\bar{\alpha}$	CuK$\bar{\alpha}$
μ (cm^{-1})	10.83	0.97	0.97	0.99	0.99	12.57	12.67
no. measd reflectns	7658	6416	6788	14434	9037	5706	3129
$2\theta_{max}$	125	60	60	60	60	124	128
forms	$\pm h \pm kl$	$\pm h \pm kl$ $(2 < \theta < 15)$ $\pm hkl$ $(13 < \theta < 30)$	$\pm hkl$	$\pm h \pm k \pm l$ $(2 < \theta < 12)$ $\pm h \pm kl$ $(12 < \theta < 25)$ $\pm hkl$ $(25 < \theta < 30)$	$\pm h \pm kl$ $(2 < \theta < 13)$ $\pm hkl$ $(13 < \theta < 33)$	$\pm h \pm k \pm l$	$\pm hkl$
no. unique reflectns	3353	5343	5443	5745	6476	2665	2648
merging R^b	0.01	0.006	0.029	0.013	0.022	0.025	0.030
no. obsd^c reflectns	3151	3243	3267	3544	3421	2214	2053
max transmission	0.82					0.92	0.95
min transmission	0.75					0.64	0.82
no. params refined	360	359	382	359	359	291	292
R	0.034	0.046	0.046	0.047	0.050	0.060	0.037
Rw	0.059	0.051	0.055	0.051	0.058	0.072	0.045
GOF	2.43	1.36	1.18	1.41	1.23	2.49	1.40
extinction parameter	0.31 (5)						0.08 (2)
max shift/error	0.002	0.05	0.04	0.05	0.02	0.003	0.08
max $\Delta\rho$ (e Å^{-3})	0.3	0.3	0.4	0.3	0.4	0.7	0.3
min $\Delta\rho$ (e Å^{-3})	−0.2	−0.2	−0.3	−0.3	−0.3	−0.3	−0.3

[a] Alternative setting of $P2_1/c$. [b] R merg = $[\sum(N\sum^{N} w(F - \langle F\rangle)^2)/\sum((N-1)\sum^{N} wF^2)]^{1/2}$. [c] $I \geq 3\sigma(I)$.

18 h at 55 °C under an atmosphere of nitrogen and then poured into brine (200 mL). The mixture was extracted with pentane (3 × 100 mL). The combined organic extracts were washed with brine (2 × 100 mL), dried ($MgSO_4$), and evaporated down to a clear oil (2.4 g). Purification by passage through a silica gel column with pentane eluant gave **15** as a colorless oil (1.8 g, 93%).

***r*-5-*tert*-Butyl-*c*-2-(trimethylsilyl)cyclohexan-*t*-ol (8).** Trimethylsilyl ether **15** (1.8 g, 6 mmol) was added to a mixture of methanol (50 mL) and anhydrous potassium carbonate (2 g). The resulting mixture was refluxed under nitrogen for 2 h then cooled and diluted with brine (200 mL). The mixture was extracted with diethyl ether (3 × 100 mL), and the combined ether extracts were washed with brine (2 × 50 mL), dried ($MgSO_4$), and evaporated down to an oil (1.6 g, 95%).

***r*-4-*tert*-Butyl-*t*-2-(trimethylsilyl)cyclohexan-*c*-ol (9).** To a stirred solution of hexamethyldisilane (7.96 g, 54 mmol) in HMPA (100 mL) at 55 °C under nitrogen was added potassium methoxide (100 mg). The solution developed a light yellow-brown color. To this mixture was added a mixture of *cis*- and *trans*-4-*tert*-butylcyclohexene oxide (3.4 g, 22 mmol) resulting in the formation of a deep red color. This solution was stirred at 55 °C for 18 h and then poured into saturated brine (500 mL) and extracted with pentane (3 × 100 mL). The combined organic extracts were washed with brine (3 × 100 mL), dried ($MgSO_4$), and evaporated down to a colorless oil (6.5 g); purification by column chromatography gave a 1:1 mixture of **15** and **16** (5.9 g, 90%) as a colorless oil which was a single spot by TLC (R_f 0.8 silica gel, pentane eluant).

A mixture of trimethylsilyl ethers **15** and **16** (3.4 g) was added to a suspension of anhydrous potassium carbonate (3 g) in dry methanol (100 mL). The resulting mixture was refluxed for 2 h under nitrogen, cooled, and diluted with brine (400 mL). The mixture was extracted with diethyl ether (3 × 100 mL). The combined organic extracts were washed with brine (2 × 50 mL), dried ($MgSO_4$), and evaporated down an oily solid (2.1 g) 81%. This showed the presence of two compounds in a roughly 1:1 ratio. Fractional crystallization of this mixture from pentane gave **9** (300 mg, 23% overall) as white needles, mp 94–96 °C. Anal. Calcd for $C_{13}H_{28}OSi$: C, 67.03; H, 12.33; Si, 12.06. Found: C, 67.33; H, 12.79; Si, 12.10.

***cis*- and *trans*-4-*tert*-Butyl-1-(trimethylsilyl) Epoxides 17.** The epoxide mixture **17** was prepared as previously described[3] giving a white solid which was purified by sublimation (100 °C (1 mmHg)), mp 39–41 °C.

Reduction of the Epoxides 17. Treatment of the epoxides **17** as previously described[3] with 1:1 $AlCl_3/LiAlH_4$ in diethyl ether gave a mixture of two compounds which were separated by column chromatography on silica gel. Crystallization of the first recovered fraction from pentane gave ***r*-5-*tert*-butyl-*t*-2-(trimethylsilyl)cyclohexan-*t*-ol (10**, 50% yield), mp 88–89 °C (lit.[3] mp 90 °C) (R_f 0.9, 20% diethyl ether/pentane). The second fraction ***r*-5-*tert*-butyl-*c*-2-(trimethylsilyl)cyclohexan-*c*-ol (11)** was obtained only as an oil (R_f 0.7, 20% diethylether/pentane, 20% yield). ^{1}H NMR as lit.[19]; IR and ^{13}C NMR data deposited.

Preparation of *trans*-2-(Trimethylsilyl)cyclohexanol (12). To a solution of hexamethyldisilane (4 g, 27 mmol) in HMPA (50 mL) stirred at 60 °C was added potassium methoxide (100 mg) resulting in the development of a dark yellow solution. To this mixture was added cyclohexene oxide (1 g, 10 mmol) whereupon the solution turned a dark red color. The resulting mixture was stirred overnight and then diluted with brine (200 mL) and extracted with pentane (3 × 50 mL). The combined pentane extracts were washed with brine (3 × 50 mL), dried ($MgSO_4$), and evaporated down to a clear oil. This oil was added to a mixture of methanol (50 mL) and anhydrous potassium carbonate (2 g) and refluxed under nitrogen for 2 h. The resulting mixture was diluted with brine (200 mL) and extracted with diethyl ether (3 × 50 mL). The combined ether extracts were washed with brine (2 × 50 mL), dried ($MgSO_4$), and evaporated down to a clear oil. This was purified by distillation (80 °C (1 mmHg)) giving **12** as a clear oil which crystallized (1.5 g, 85% yield), mp 49–50 °C (lit.[3] mp 48–50 °C).

Preparation of *cis*-2-(Trimethylsilyl)cyclohexanol (13). The *cis*-2-(trimethylsilyl)cyclohexanol was prepared by the previously reported method.[3]

Preparation of the Esters 1–7. Preparation of the model ester compounds was carried out by the general procedure described for the preparation of **1**, except that in the case of the 3,5-dinitrobenzoate ester **3**, 3,5-dinitrobenzoyl chloride was used instead of *p*-nitrobenzoyl chloride.

***r*-5-*tert*-Butyl-*c*-2-(trimethylsilyl)cyclohex-*t*-yl *p*-Nitrobenzoate (1).** To a solution of *p*-nitrobenzoyl chloride (0.07 g, 0.38 mmol) in pyridine (5 mL) was added a solution of the alcohol **10** (0.07 g, 0.31 mmol) in pyridine (1 mL). The resulting suspension was stirred overnight at room temperature and then diluted with water (50 mL). The mixture was extracted with methylene chloride (3 × 20 mL) and the combined extracts washed with 1 M HCl (2 × 50 mL), water (2 × 50 mL), and aqueous sodium bicarbonate (1 × 50 mL), dried ($MgSO_4$), and evaporated down to a pale yellow solid. Recrystallization from pentane gave **1** as colorless rods (0.104 g, 90%), mp 119–120 °C.

***r*-4-*tert*-Butyl-*t*-2-(trimethylsilyl)cyclohex-*c*-yl *p*-Nitrobenzoate (2).** White blocks from pentane (91%), mp 121–121.5 °C.

***r*-4-*tert*-Butyl-*t*-2-(trimethylsilyl)cyclohex-*c*-yl 3,5-Dinitrobenzoate (3).** White blocks from pentane (0.27 g, 95%), mp 111–112 °C.

***r*-5-*tert*-Butyl-*t*-2-(trimethylsilyl)cyclohex-*t*-yl *p*-Nitrobenzoate (4).** White needles from pentane (0.5 g, 90%), mp 143–144 °C.

***r*-5-*tert*-Butyl-*c*-2-(trimethylsilyl)cyclohex-*c*-yl *p*-Nitrobenzoate (5).** White rods from pentane (0.3 g, 91%), mp 99–100 °C.

***cis*-2-(Trimethylsilyl)cyclohexyl *p*-Nitrobenzoate (6).** White needles from pentane (96%), mp 82–82.5 °C.

***trans*-2-(Trimethylsilyl)cyclohexyl *p*-Nitrobenzoate (7).** Off-white needles from pentane (0.38 g, 92%), mp 53–54 °C.

(b) Crystallography. Diffraction data were recorded with a Philips PW1100/20 diffractometer operating in θ–2θ continuous scan mode. Crystal temperatures were maintained at 130 ± 2 K with a Leybold–Heraeus nitrogen cooling device. Data were reduced to F_o and σ (F_o) as described elsewhere[20] with absorption corrections (for Cu Kα data only) calculated using Gaussian quadrature.[21] Structures were solved by direct methods (SHELXS)[22] and were refined with CRYLSQ[23] [full-matrix least-squares analysis on *F*; reflection weights = $[\sigma(F_o)^2 + 0.0005\,(F_o)^2]^{-1}$; H-atoms isotropic, non-H atoms anisotropic]. The isotropic extinction correction of Zachariasen[24] was applied when appropriate. Crystal data, together with data collection/refinement details, are listed in Table III.

Supplementary Material Available: Tables of atomic coordinates and thermal parameters, bond lengths, and interbond angles and NMR and IR data (49 pages). This material is contained in many libraries on microfiche, immediately follows this article in the microfilm version of the journal, and can be ordered from the ACS; see any current masthead page for ordering information.

---

(19) Fristad, W. E.; Bailey, T. R.; Paquette, L. A. *J. Org. Chem.* **1980**, *45*, 3028.

(20) Robertson, G. B.; Whimp, P. O. *J. Am. Chem. Soc.* **1975**, *97*, 1051.

(21) Sheldrick, G. M. *SHELX-76, Program for Crystal Structure Determination*; University of Cambridge: Cambridge, England, 1976.

(22) SHELXS-86: Sheldrick, G. M. *Crystallographic Computing 3*; Sheldrick, G. M., Krüger, C., Goggard, R., Eds.; Oxford University Press, Oxford, England, 1985; pp 175–189.

(23) Olthof-Hazekamp, R. *CRYLSQ, XTAL 2.6 Users Manual*; Hall, S. R., Stewart, J. M., Eds.; Universities of Western Australia and Maryland, 1989.

(24) Zachariasen, W. H. *Acta Crystallogr.* **1963**, *16*, 1139.